

Fabrication of solid-state nanopores with single-nanometre precision

A. J. STORM¹, J. H. CHEN^{1,2}, X. S. LING^{1,3}, H. W. ZANDBERGEN¹ AND C. DEKKER^{*1}

¹Department of NanoScience, Delft University of Technology, 2628 C.J. Delft, The Netherlands

²Netherlands Institute for Metals Research, 2628 AL Delft, The Netherlands

³Permanent address: Department of Physics, Brown University, Providence, Rhode Island 02912, USA

*e-mail: dekker@mb.tn.tudelft.nl

Published online: 13 July 2003; doi:10.1038/nmat941

Single nanometre-sized pores (nanopores) embedded in an insulating membrane are an exciting new class of nanosensors for rapid electrical detection and characterization of biomolecules. Notable examples include α -hemolysin protein nanopores in lipid membranes^{1,2} and solid-state nanopores³ in Si_3N_4 . Here we report a new technique for fabricating silicon oxide nanopores with single-nanometre precision and direct visual feedback, using state-of-the-art silicon technology and transmission electron microscopy. First, a pore of 20 nm is opened in a silicon membrane by using electron-beam lithography and anisotropic etching. After thermal oxidation, the pore can be reduced to a single-nanometre when it is exposed to a high-energy electron beam. This fluidizes the silicon oxide leading to a shrinking of the small hole due to surface tension. When the electron beam is switched off, the material quenches and retains its shape. This technique dramatically increases the level of control in the fabrication of a wide range of nanodevices.

The fabrication of our 20 nm to 200 nm pores in silicon oxide builds on earlier work⁴ by Gribov *et al.* Silicon-on-insulator (SOI) wafers with a top single-crystal silicon layer of 340 nm with crystal orientation $\langle 100 \rangle$ were used to fabricate $70 \times 70 \mu\text{m}^2$ free-standing silicon membranes, using micromachining techniques. The membranes are thermally oxidized on both sides with a SiO_2 layer of 40 nm thickness. Using electron-beam lithography and reactive-ion etching we open squares with dimensions up to 500 nm in the SiO_2 mask layer at the top. Subsequently, pyramid-shaped holes are etched using anisotropic KOH wet etching. Stripping the 40-nm oxide in buffered hydrogen fluoride opens up the pore in the silicon membrane (see Fig. 1a). The last processing step is a thermal oxidation to form a SiO_2 surface layer with a thickness of 40 nm. Figure 1b shows a top-view scanning electron micrograph (from a Philips/FEI XL30S SEM) of the pore after the fabrication process. Each device used in the experiments reported here contains a silicon membrane with up to 400 pyramid-shaped holes with various dimensions, from closed pores to pores of about 200 nm.

In this letter we report a new technique to fine-tune the size of pores with nanometre precision. Our main tool here is a commercial transmission electron microscope (TEM), a Philips CM-30UT operated at an accelerating voltage of 300 kV. It is well known in electron microscopy that a high electron intensity can damage or deform the specimen, and in general one tries to minimize this effect. However, we

use this effect to modify the dimensions of our silicon oxide nanopores in a well-controlled way. Figure 1c shows a cross-section view of a nanofabricated pore in the microscope. We found that an electron beam of intensity around 10^5 to 10^7 A m^{-2} causes pores to shrink if the pore had an initial diameter of about 50 nm or lower. Remarkably, different dynamics were found for pores with initial dimensions of about 80 nm or higher. These pores expand in size instead of the shrinking dynamics observed for small pores. The changes in pore diameter can be monitored in real-time using the imaging mechanism of the microscope. Figure 1d–g shows a sequence of images obtained while imaging a pore with an initial diameter of 19 nm. A movie in the Supplementary Information shows a closing pore during TEM imaging. The surprising effect of growing and shrinking pores can be understood from surface tension effects in the viscous silicon oxide, as discussed below.

The hole closing reported in this letter is certainly not caused by deposition of carbon-rich material by the electron beam, a common phenomenon in electron microscopy. The observation that large pores expand is in direct contradiction with potential contamination growth. Secondly, electron-energy-loss spectra (EELS) locally obtained on the material that filled a nanopore clearly show the presence of silicon and oxygen, but the absence of any carbon (detection limit was less than 2%).

The power of our technique lies in the possibility of fine-tuning the diameter of nanopores with unprecedented precision. By lowering the beam intensity or blanking it, the shrinking process can be stopped within seconds when the desired diameter has been reached. Figure 2 shows the average diameter of the pore versus time. In this experiment, the diameter of the pore shrinks at a rate of about 0.3 nm per minute, slow enough to stop at any desired dimension. If favoured, coarse shrinking can be done at least an order of magnitude faster by increasing the electron intensity, and can gradually be slowed down for ultimate control. The final precision is limited by the resolution of the microscope (0.2 nm for ours). In practice, the resolution is limited to about 1 nm due to the surface roughness of the silicon oxide. The level of control is at least an order of magnitude better than conventional electron-beam lithography, which has an ultimate resolution of about 10 nm. Our technique drastically limits the required dimensional control in the prior lithographic process, because any pore with a diameter below 50 nm can be shrunk to a nanometre-sized pore.

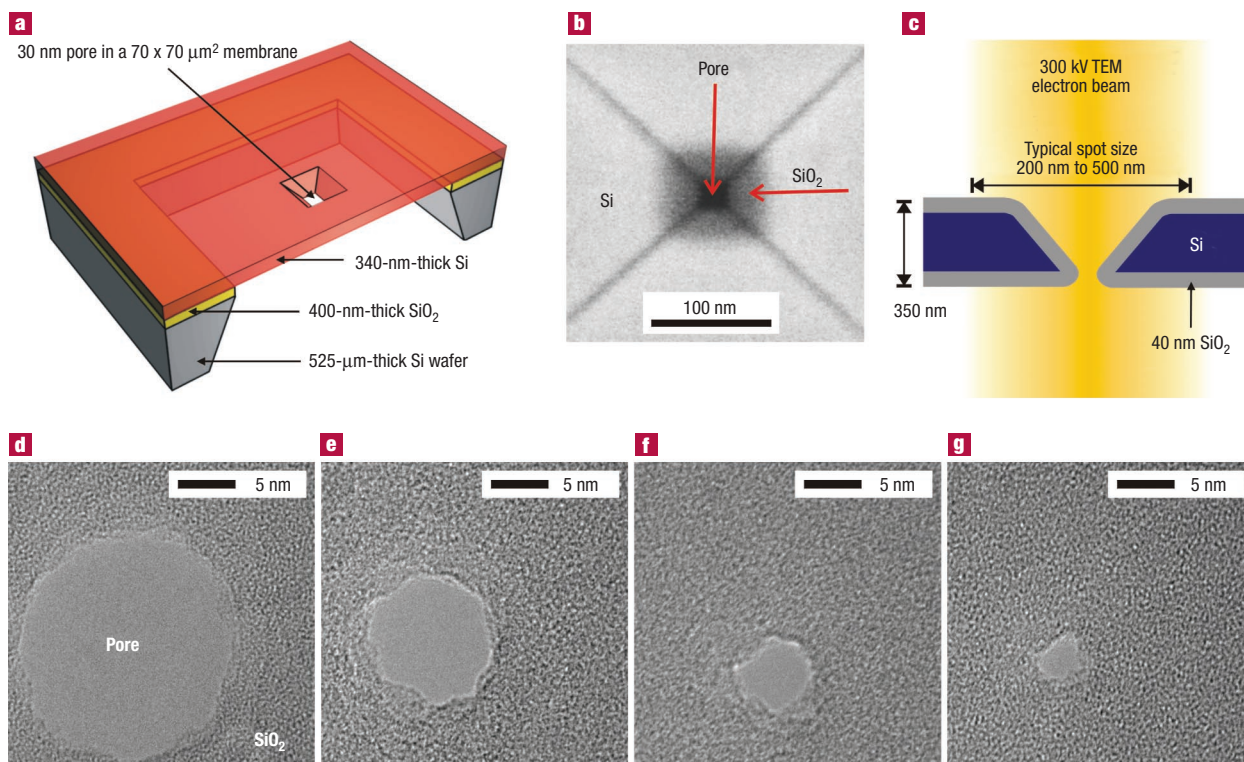


Figure 1 Fabrication of silicon oxide nanometre-sized pores **a**, Cross-section view of our device. It consists of a 340-nm-thick free-standing single-crystalline silicon membrane, supported by a KOH-etched wafer 525 μm thick. The membrane contains one or more submicrometre, pyramid-shaped pores, anisotropically etched with KOH from the top. **b**, Top-view scanning electron micrograph of a nanofabricated pore after thermal oxidation. The pore is about $20 \times 20 \text{ nm}^2$, and is surrounded by a SiO_2 layer of about 40 nm thickness. **c**, Cross-sectional view of the pore inside the electron microscope. **d–g**, Sequence of micrographs obtained during imaging of a silicon oxide pore in a TEM microscope. The electron irradiation causes the pore to shrink gradually to a size of about 3 nm.

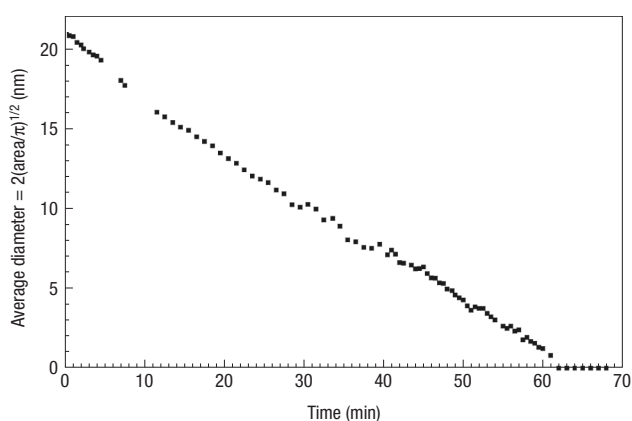


Figure 2 Diameter versus time for a shrinking pore with an initial size of about 21 nm. A sequence of TEM micrographs was obtained using a charge-coupled-device camera during continuous electron irradiation at constant intensity and focus setting. From each image we estimated the area from a polygon tracing the perimeter of the pore. This area was used to calculate the diameter of the pore assuming a circular shape. The absolute error in this measurement is estimated to be 1 nm, which, to a large extent is due to the width of the diffraction ring around the perimeter of the pore.

The fabricated pores were found to be stable at ambient conditions and in water.

The pore-size tuning technique was further tested on holes fabricated using a different process. In agreement with Chen *et al.*⁵, we find that a focused electron beam with a spot size of a few nanometres can be used to drill holes in thin free-standing SiO_2 membranes, with an estimated thickness of about 10 nm (Fig. 3a). Figure 3b,c shows a pore that has been drilled using an electron-beam intensity above $1 \times 10^8 \text{ A m}^{-2}$. Holes as small as 6 nm can be obtained, but this technique does not give full control at the nanometre scale because no images can be recorded during drilling. It is however possible to subsequently fine-tune the size of the drilled pores using the same process as discussed earlier, if the diameter is small enough. As a demonstration, Fig. 3d–f shows a sequence of micrographs where a 6 nm pore is reduced down to 2 nm. At the high exposure levels necessary for drilling the hole, the oxygen content of the silicon oxide irradiated by the electrons was strongly reduced⁶. Energy-dispersive X-ray (EDX) analysis shows up to 80% oxygen depletion during hole drilling. It should be noted that the irradiation levels needed for the controlled pore shrinking are about a factor 100 lower than those used for the hole drilling. EDX experiments at these lower intensities show oxygen depletion rates of less than 10% per hour.

The effect of electron irradiation at intensities between 10^5 and 10^7 A m^{-2} on amorphous SiO_2 has not yet received much attention. Based on the apparent morphological changes in our nanostructures on imaging, and the absence of changes in the composition of the irradiated material, we conclude that at these electron irradiation levels viscous

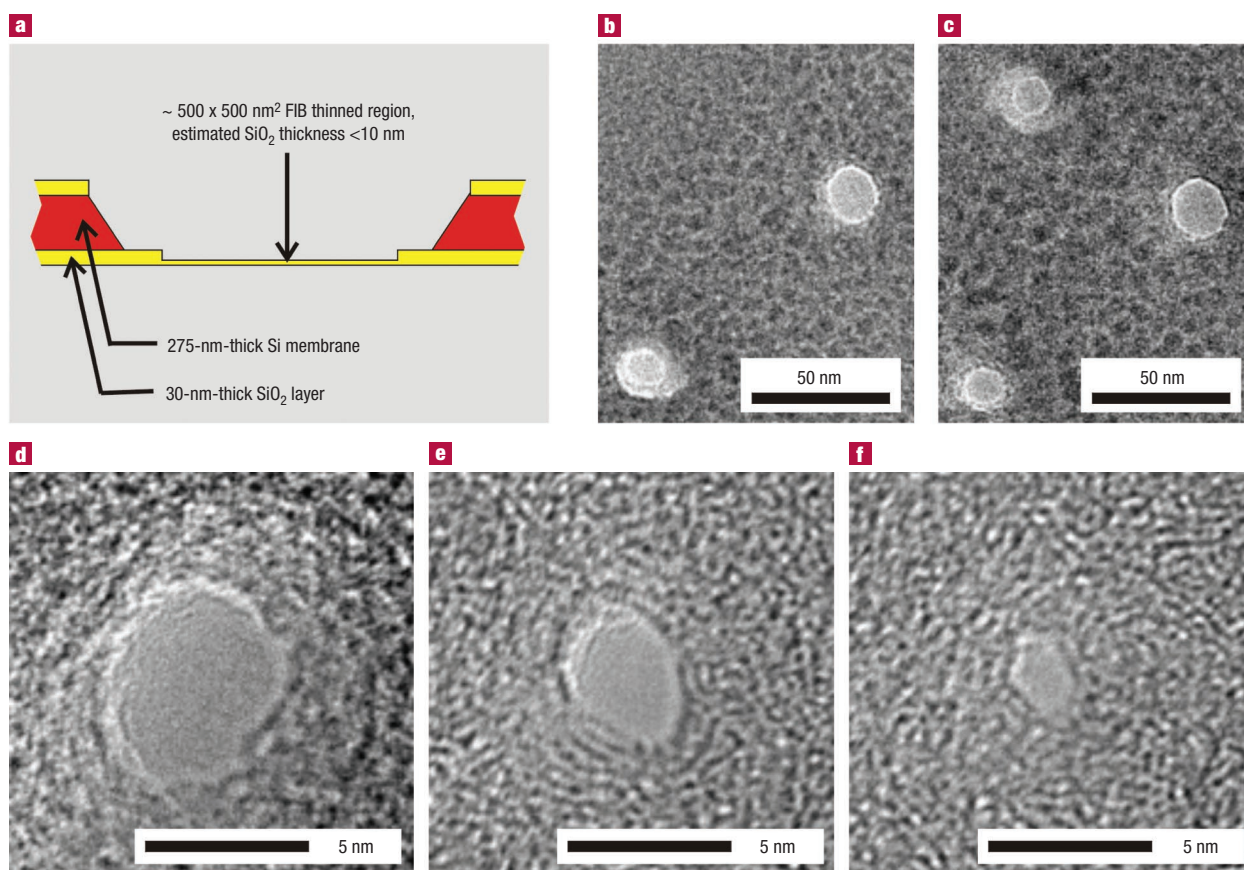


Figure 3 TEM-drilled nanopores in thin free-standing SiO_2 membranes. **a**, Cross-section of a thin SiO_2 membrane within a silicon-based membrane. Fabrication of this structure starts with a bare silicon membrane, which is oxidized with about 30 nm of SiO_2 on both sides. Using electron-beam lithography and reactive-ion etching we open up $1 \times 1 \mu\text{m}^2$ squares in the oxide layer. After a KOH wet etch, we obtain 30-nm-thick SiO_2 membranes. Subsequently these were thinned further in a focused ion-beam (FIB) microscope (FEI Strata DB235), to a final estimated thickness of less than 10 nm. **b**, TEM micrograph of a part of a membrane with two holes that were drilled by a finely focused electron beam inside the TEM microscope. **c**, TEM micrograph after drilling a third hole in the membrane depicted in Fig. 3b. **d–f**, Sequence of TEM images obtained on a shrinking nanopore with an initial diameter of about 6 nm and a final diameter of only 2 nm.

flow is induced in the amorphous silicon oxide, in agreement with observations seen previously⁷. Whereas the electron beam clearly provides the energy to soften the material, direct specimen heating alone does not explain the effect⁷. At intensities above 10^7 A m^{-2} another mechanism dominates, and oxygen is preferentially lost from the silicon oxide. Radiation with an electron beam focused to a spot of a few nanometres leads to formation of pure silicon structures at the nanometre scale⁶, and prolonged irradiation eventually leads to the formation of a hole in thin films⁵.

The physics of the observed growing and shrinking of nanopores is determined by the surface tension of the viscous silicon oxide. In the fluidized state, the structure will deform to find a configuration with a lower surface free energy F . For simplicity we model our pore as cylindrical with radius r in a sheet of material with constant thickness h , see Fig. 4a. The change in free energy compared with an intact sheet is $\Delta F = \gamma \Delta A = 2\pi\gamma(rh - r^2)$, where γ is the surface tension of the liquid, and ΔA is the change in surface area. From the graph $\Delta F(r)$ in Fig. 4b, it can be seen that pores with radius $r < h/2$ can lower their surface free energy by reducing r , whereas pores with radius $r > h/2$ do so by increasing size. The ‘critical diameter’ $2r$ discriminating the two cases is of order of the thickness of the sheet, with the exact value depending on the geometry of the pore. This scaling argument is valid at any scale,

and elegantly explains the observed dynamics in our pores. We estimate that in our SOI pores the effective height of the pore is about 40 nm, the thickness of the silicon oxide layer, in good agreement with the observed ‘critical diameter’ between 50 nm and 80 nm in our experiments. In the experiments on holes in thin silicon oxide films, we observed a much lower critical diameter of around 10 nm, in agreement with the model.

Similar dynamics and interpretations were described⁸ for holes in films of mercury on the millimetre scale investigated by optical microscopy. Similar effects on nanometre-sized holes in 20-nm-thick crystalline gold films have been studied before and after annealing⁹. Again the interpretation is surface-tension-driven mass flow. Direct comparison of our results to the TEM work of Ajayan and Iijima⁷ shows that the deformation rate is a factor of 10 to 100 slower in our work, which is a striking difference because the material and radiation conditions are similar in both experiments. This apparent discrepancy can be explained from a consideration of the geometry. A curved liquid surface will generate a Laplace pressure inversely proportional to the radius of curvature. The tips described by Ajayan and Iijima had a radius of curvature of the order of 1 nm, whereas our pores have a typical curvature of about 10 nm, leading to lower pressures and slower dynamics.

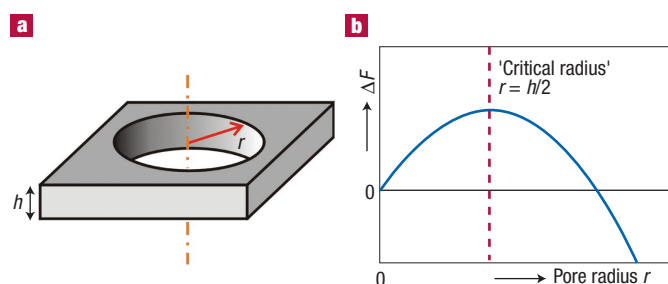


Figure 4 A model system explaining nanopore shrinking and expanding dynamics. **a**, We model our system as a cylindrical pore with radius r in a sheet of liquid with thickness h . **b**, Change of surface free energy on formation of a cylindrical pore in a liquid film. From the graph $\Delta F(r)$ can be seen that pores with radius $r < h/2$ can lower their surface free energy by reducing r , and pores with radius $r > h/2$ by increasing r .

In summary, we have demonstrated a new method to make solid-state nanopores with single-nanometre precision. The advantage of this technique is that nanometre-scale sample modifications are possible with direct visual feedback at subnanometre resolution. The process is based on standard silicon processing and commercially available TEM microscopes. A modest resolution of about 50 nm is required in the lithography defining the pore, as fine-tuning in the electron beam is done as a final step. Using the SOI-based process, it is straightforward to obtain this requirement with electron-beam lithography, and should be attainable even with optical lithography alone. A recent report³ on 'ion beam sculpting' of nanopores showed, for the first time, a process for controlled fabrication of pores in silicon nitride, and demonstrated the potential of inorganic nanopores for DNA analysis on the single-molecule level. Our technique has the additional advantages of direct visual feedback, as well as the fact that it does not change the chemical

composition of the material surrounding the pore. In a way, our technique is like glassblowing at the nanoscale: we use the electron beam to soften the glassy silicon oxide, allowing it to deform slowly driven by the surface tension. The electron microscope provides real-time visual feedback, and when the desired morphology has been obtained the electron beam intensity is lowered and the silicon oxide is quenched to its initial glassy state. This technique can greatly increase the level of control in a wide range of nanotechnological applications: nanopore devices for biomolecular analysis, metallic point contacts and electrodes for molecular electronics.

Received 24 March 2003; accepted 6 June 2003; published 13 July 2003.

References

1. Kasianowicz, J. J., Brandin, E., Branton, D. & Deamer, D. W. Characterization of individual polynucleotide molecules using a membrane channel. *Proc. Nat. Acad. Sci. USA* **93**, 13770–13773 (1996).
2. Howorka, S., Cheley, S. & Bayley, H. Sequence-specific detection of individual DNA strands using engineered nanopores. *Nature Biotechnol.* **19**, 636–639 (2001).
3. Li, J. *et al.* Ion-beam sculpting at nanometre length scales. *Nature* **412**, 166–169 (2001).
4. Gribov, N. N., Theeuwes, S. J. C. H., Caro, J. & Radelaar, S. A new fabrication process for metallic point contacts. *Microelectron. Eng.* **35**, 317–320 (1997).
5. Chen, G. S., Boothroyd, C. B. & Humphreys, C. J. Electron-beam-induced damage in amorphous SiO_2 and the direct fabrication of silicon nanostructures. *Phil. Mag. A* **78**, 491–506 (1998).
6. Chen, G. S., Boothroyd, C. B. & Humphreys, C. J. Novel fabrication method for nanometre-scale silicon dots and wires. *Appl. Phys. Lett.* **62**, 1949–1951 (1993).
7. Ajayan, P. M. & Iijima, S. Electron-beam-enhanced flow and instability in amorphous silica fibres and tips. *Phil. Mag. Lett.* **65**, 43–48 (1992).
8. Taylor, G. I. & Michael, D. H. On making holes in a sheet of fluid. *J. Fluid. Mech.* **58**, 625–639 (1973).
9. Lanxner, M., Bauer, C. L. & Scholz, R. Evolution of hole size and shape in {100}, {110} and {111} monocrystalline thin films of gold. *Thin Solid Films* **150**, 323–335 (1987).

Acknowledgements

We thank P. F. A. Alkemade, E. W. J. M. van der Drift, J. Jansen, J. Prost, D. M. Stein and M. Zuiddam for technical assistance and fruitful discussions. This work was financially supported by the Dutch Foundation for Fundamental Research on Matter (FOM). X.S.L. wishes to thank the John Simon Guggenheim Foundation for support.

Correspondence and requests for materials should be addressed to C.D.

Supplementary Information accompanies the paper on www.nature.com/naturematerials

Competing financial interests

The authors declare competing financial interests: details accompany the paper on www.nature.com/naturematerials

MOVIE CAPTION:

Shrinking a nanopore in silicon oxide using a TEM microscope.

This movie shows a sequence of TEM micrographs displayed 25 times faster than the original recording rate. The initial diameter of 26 nm was reduced down to 2 nm in about 10 minutes.